Dalton Transactions

Accepted Manuscript

This article can be cited before page numbers have been issued, to do this please use: Y. Sun, C. Shi and W. Zhang, *Dalton Trans.*, 2017, DOI: 10.1039/C7DT03798H.

ROYAL SOCIETY OF CHEMISTRY

rsc.li/dalton

View Article Online
DOI: 10.1039/C7DT03798H

Journal Name

COMMUNICATION

Distinct room-temperature dielectric transition in a perchlorate-based organic-inorganic hybrid perovskite

Received 00th January 20xx,
Accepted 00th January 20xx

DOI: 10.1039/x0xx00000x

www.rsc.org/

Yu-Ling Sun, Chao Shi and Wen Zhang*

Organic-inorganic hybrid perovskite $(H_2hpz)[K(ClO_4)_3]$ (H_2hpz = diprotonated homopiperazine) exhibits a distinct room-temperature dielectric transition. The dielectric switching at 303 K is associated with an order-disorder transition of the polar guest cation confined in the cage, corresponding to a dynamic change between motional and frozen states.

Responsive/smart materials can change physical and chemical properties under external stimuli and have been widely used.[1-5] Exploration of new responsive materials has been greatly desired as the case of switchable dielectric materials.[5-12] This new type of responsive electrical materials is characterized by dielectric transitions between high- and low-dielectric states upon external stimuli such as temperature, pressure and light.[5] They are different from conventional constant or static dielectric materials and have potential applications in smart electrical and electronic devices, such as switches, sensors, varactors and actuators.

The microscopic origin of the dielectric switching in molecular materials is usually associated with structural phase transition which is triggered by the motional changes of the dipoles, e.g., rotating or hopping in the high-temperature phase (high-dielectric state) and frozen in the low-temperature phase (low-dielectric state).[5,13] The phase transition temperature (T_{tr}) is the switching temperature of the dielectric constant. Therefore, tuning the local dipolar orientation is the key to construct switchable dielectrics. This is presently still a hard task because the local motional states of the polar molecules in the crystal lattice are controlled by their surroundings via intermolecular interactions which we have still known little. Fortunately, such a difficulty can be largely circumvented by screening some typical model systems. One is the host-guest type of organic-inorganic hybrid frameworks, in which the properly designed host cavity tunes the dipolar orientations of the confined polar guest, resulting in the desired dielectric switching.[6-11] The mostly studied frameworks are the organic-inorganic hybrid perovskites ABX_3 in which the bridging ligand X is commonly monodentate, e.g., halide ion, $HCOO^-$, CN^-, N_3^- and the like.[12] It is found that the cavities in the perovskite structures and the dynamics of the confined guest A can be primarily modified by the X and finely tuned by B.[6,9]

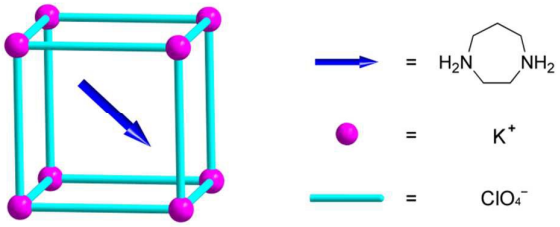

Scheme 1. Schematic illustration of the basic cage unit of the hybrid perovskite **1**.

In our previous study, we reported a new series of hybrid perovskites by introducing ClO_4^- and BF_4^- as the bridging ligand.[14] Different from the commonly used linear or V-shaped bridging ligands which are monodentate and generally six-coordinated with the B metal ion, the ClO_4^- and BF_4^- ligands are tetrahedral and can exhibit monodentate and/or chelating coordination modes with the B ion. When the guest is diprotonated 1,4-diazabicyclo[2.2.2]octane or piperazine, the corresponding compounds exhibit order-disorder phase transitions and dielectric responses. However, the dielectric changes are small at T_{tr} because of the guest cations are nonpolar and there is no net contribution from dipolar orientations. Herein, we introduce a polar cationic guest, diprotonated homopiperazine (H_2hpz), as the A-site organic cation to construct a new hybrid perovskite $(H_2hpz)[K(ClO_4)_3]$ (**1**) (Scheme 1). With the contribution from the dipolar orientation of the H_2hpz guests, a striking dielectric switching is realized at 303 K.

Compound **1** was obtained as block crystals by an evaporation method. Thermogravimetric analysis indicates it keeps stable below 540 K (Figure S1). Differential scanning calorimetry (DSC) measurement shows that **1** undergoes three reversible phase transitions at 306/299 K (T_{tr1}), 330/330 K (T_{tr2}) and 358/356 K (T_{tr3}) upon a heating-cooling cycle (Figure 1 and S2). The corresponding thermal hystereses are 7 K (T_{tr1}), 0 K (T_{tr2}) and 2 K (T_{tr3}) at a scanning rate of 20 K min^{-1}. For

Ordered Matter Science Research Center, Southeast University, Nanjing 211189, Jiangsu, China. E-mail: zhangwen@seu.edu.cn
† Electronic Supplementary Information (ESI) available. See DOI: 10.1039/x0xx00000x

View Article Online
DOI: 10.1039/C7DT03798H

convenience, the room-, intermediate- and high-temperature phases (RTP, ITP and HTP) are assigned to the phases below the T_{tr1}, between the T_{tr1} and T_{tr3}, and above the T_{tr3}, respectively. Below and above the T_{tr2}, the ITP is further divided into ITP α and ITP β. The corresponding entropy changes (ΔS) are 15.6, 0.31 and 1.79 J·mol^{-1}·K^{-1} for the RTP-ITP α, ITP α-ITP β and ITP β-HTP transitions, respectively. The corresponding microscopic state change N is estimated to be 6.54 (303 K), 1.04 (330 K) and 1.24 (357 K) by using the Boltzmann equation ΔS = R ln N, suggesting a characteristic of order-disorder type of the RTP-ITP α phase transition in **1**.

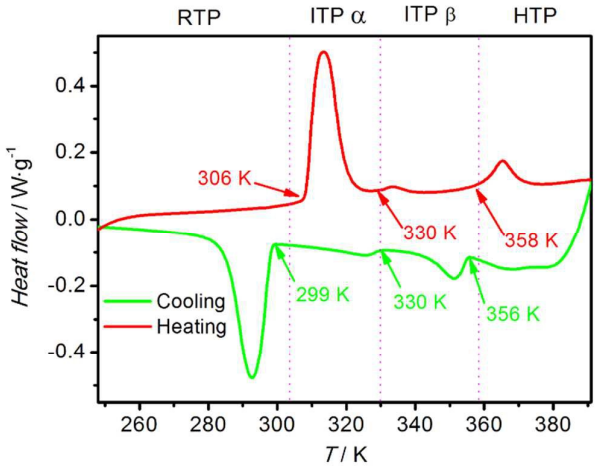

Figure 1. DSC curve of **1** measured in a heating-cooling cycle with a scanning rate of 20 K min^{-1}.

Structural phase transitions in **1** was characterized by variable-temperature X-ray diffraction (Figure 2 and Table S1). The perovskite structure is composed of K^+ nodes and ClO_4^- linkers to form anionic cages in which the H_2hpz cations reside. In the RTP at 203 K, **1** crystallizes in the orthorhombic space group *Pbca* with a = 9.603(3) Å, b = 14.769(5) Å, c = 20.786(7) Å and V = 2948 Å^3. In the host cage, the K^+ ion is hendecahedrally coordinated by six ClO_4^- ligands with K–O distances between 2.749–3.308 Å (Table S2), among which there is only one ClO_4^- group (Cl1) acting as a monodentate ligand and the other five acting as bidentate ligands. The anionic cage is relatively largely distorted with different K···K distances (7.017–7.433 Å) and K···K···K angles (85.62–94.49°). The H_2hpz cation resides in the cage and adopts a completely ordered state. It shows a chair-like conformation (Figure S3) The $-NH_2$ groups of the cation develop one linear, two bifurcate and one trifurcate N–H···O hydrogen bonds with the O atoms of the bridging ligands (Figure 2a and Table S3). In the packing structure, the ordered cations show eight different orientations in the cages (Figure 3a). It is notable that the three-dimensional perovskite structure has a (6,6)-connected pcu topology with the Schläfli symbol of (4^{12}·6^3).[15]

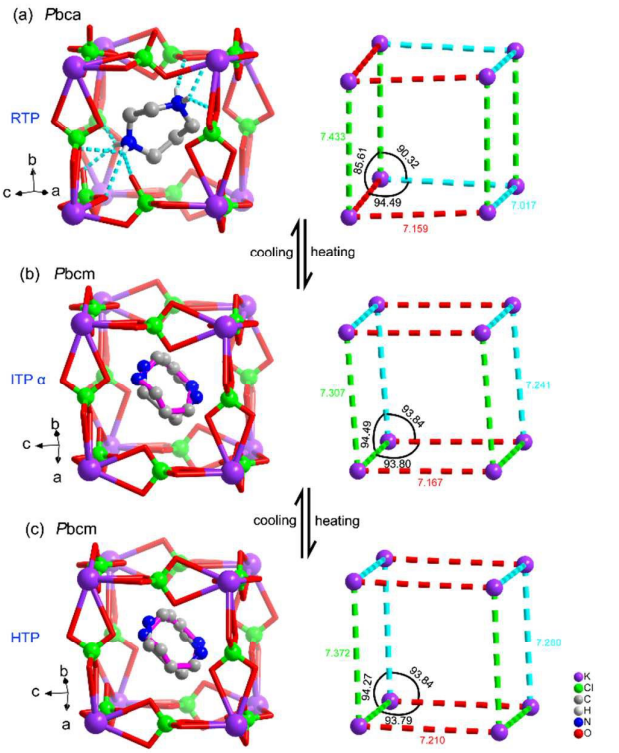

Figure 2. Cage-like structural unit of **1** in the (a) RTP, (b) ITP α and (c) HTP. Cyanic dotted lines in the left panel of (a) represent hydrogen bonds between the cations and the host cage. Distortion of the cage is depicted by the K^+ vertices with the K···K distances (Å) and K···K···K angles (°). The cations in (b) and (c) are disordered and shown in two different colors. Methylene H atoms are omitted for clarity.

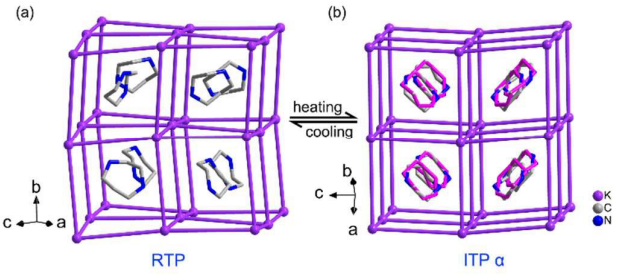

Figure 3 Schematic illustration of the pcu topology of the host and orientations of the confined cation guests of **1** in the (a) RTP and (b) ITP α. The ClO_4^- bridging ligands are presented by violet sticks. H atoms are omitted for clarity.

In the ITP α (328 K), the crystal still crystallizes in the same system as the RTP but with the space group *Pbcm*. Compared with the RTP, the cell parameters change distinctly with a = 10.682(10) Å, b = 9.876(10) Å, c = 14.264(14) Å and V = 1505 Å^3. One axis is halved and so is the volume. The K^+ ion, located on a special site with a mirror symmetry (Figure S4), is dodecahedrally coordinated by six ClO_4^- ligands in the bidentate mode. The anionic cage becomes more regular than the RTP with the slightly varied K···K distances (7.167–7.307 Å) and K···K···K angles (93.80–94.49°) (Figure 2b). The H_2hpz

DOI: 10.1039/C7DT03798H

cation in the cage becomes disordered and modelled over two sites with equal occupancies which are related by a twofold rotation axis across the C3 atom of the ring, indicating an roughly in-plane motion of the H_2hpz cation as demonstrated by following dielectric measurement. Due to the dynamic motion, the cations show two different orientations in the cages. The averaged ring planes defined by the C1, C3, C4 and C5 atoms lie in the (013) and (0$\bar{1}$3) planes with a dihedral angle of 51° (Figure 3b). Meanwhile, parts of the O atoms of the ClO_4^- groups also show relatively large thermal ellipsoids due to thermal vibrations (Table S4).

Although the structural information of **1** in the ITP β has not been obtained due to poor diffraction data, the successfully solved structure in the HTP (378 K) can contribute to a better understanding of the ITP-HTP transition. The structure at 378 K adopts the same space group as the ITP α with slight increases of the cell parameters (Table S1). The anionic framework shows no obvious changes of the K···K···K angles and only slightly elongation of the K···K distances (Figure 2c). The H_2hpz cation still remains positionally disordered in the cage. In addition, the vibration amplitude of all O atoms increases in the HTP, leading to larger thermal ellipsoid than the ITP α (Table S4). The cavity volume, calculated by PLATON,[16] increases from 124.3 Å^3 at 203 K, 130.9 Å^3 at 328 K to 134.8 Å^3 at 378 K.

Variable-temperature powder X-ray diffraction measurements were also performed on **1** to further verify the phase transitions (Figure S5). The pattern at 298 K, corresponding to the RTP of **1**, is consistent with the simulated one of single-crystal data. With the increase of the temperature, the diffraction peaks change at 340 K in the ITP with the disappearance of some peaks between 14° and 36°. There are no distinct changes of the patterns between the ITP and HTP, except for the gradual decrease of the peak intensity upon heating. These results are consistent with the single-crystal diffraction analysis.

The dielectric switching in **1** is clearly confirmed by temperature-dependent dielectric measurements on single-crystal and powder samples. The single-crystal has the largest face of the *b* plane or [010] direction (Figure S6). Along the *b* axis, the ε' of relative complex permittivity ε ($\varepsilon = \varepsilon' - i\varepsilon''$, where ε' is the real part and ε'' the imaginary part) shows a striking step-like transitions at 309/303 K upon a heating-cooling cycle, consistent with the DSC data (Figure 4a). The value of ε' remains at about 8.4 below the T_{tr1} and then increases abruptly to about 18.3 above the T_{tr1}, corresponding to the low- and high-dielectric states, respectively. It is noteworthy that the relatively large ε' in the ITP and HTP, indicating that there is a polar orientation contribution to the ε', in contrast to the analogues containing nonpolar guests that only show slight dielectric changes.[14] Above the T_{tr1}, the ε' keeps a gradual decrease as a result of the competition between polar orientation and thermal disturbance.[6] The dielectric changes show no dielectric relaxation behaviour, indicating fast motions of the guest beyond the measured frequency range. The powder sample shows a switching of the ε' between about 6 and 10 at 1 MHz around the T_{tr1}, indicating an averaged result of the anisotropic ε' (Figure S7). From the frequency-dependent dielectric constant curves (Figure S8), it is found that the ε' values decrease slowly with the increase of frequency at selected temperatures. The change values of ε' is much smaller in the high frequency, indicating that there is no dielectric dispersion.[17] The sudden increase of the ε' from 293 K to 308 K reflects the occurrence of the RTP-ITP transition.

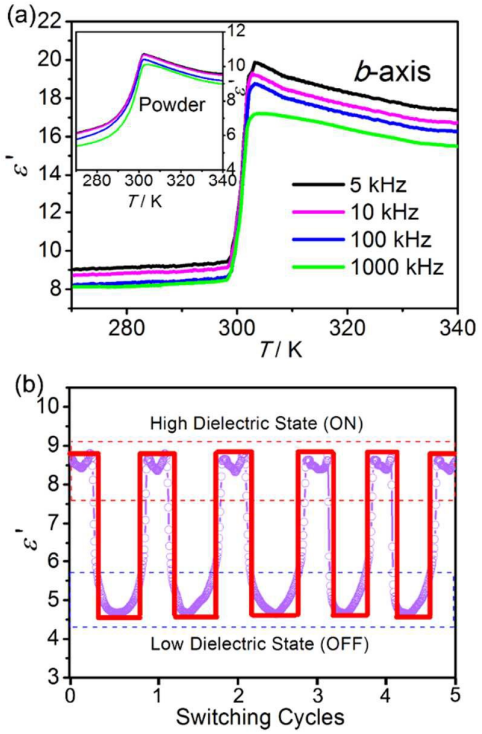

Figure 4. (a) Temperature dependence of ε' of **1** measured on single-crystal sample along the *b* axis at 1 MHz and 5–1000 kHz in a cooling run (Inset: powder sample); (b) Cycles of switching on and off of the ε' between 293–340 K and at 1 MHz.

Furthermore, reversibility of the dielectric switching between the high-dielectric state (switch on) and low-dielectric state (switch off) at 1 MHz is demonstrated by measuring polycrystalline sample in several sequential cycles (Figure 4b). The switching ratio between the high- and low-dielectric states is larger than 2. There is no observable weakening of the dielectric signal during the cycling process, indicating the compound is a room-temperature switchable dielectric material and would find potential applications in electrical responsive devices.[7c,18]

Considering the polar guest, the dipole moment of the free H_2hpz cation is 2.19 D calculated by DFT 3-21G method (Figure S9). The confined cation has nearly the same chair-like conformation and a dipole moment of 2.20 D, indicating a relative rigidity of the backbone of the guest. In the ITP and HTP, the cation undergoes dynamic disorders in the cage with possible hopping/rotating motions based on the crystallographic analysis. The details of the molecular

View Article Online
DOI: 10.1039/C7DT03798H

dynamics need further studies. The dynamics is a feature of amphidynamic crystals in which there are both motional and static components in the crystal lattices.[19] This type of crystals has a close relationship to crystalline molecular rotors or compasses.[6c,20,21]

In summary, a ClO_4^- bridging ligand based organic-inorganic hybrid perovskite $(H_2hpz)[K(ClO_4)_3]$ is synthesized by introducing a polar guest, diprotonated homopiperazine. The guest cation undergoes an order-disorder transition at 303 K due to the dynamic change between the motional and frozen states, which leads to the distinct dielectric switching. This finding demonstrate the tunability of the dielectric switchable materials with desirable properties.

This work was financially supported by the NSFC (Grant No. 21225102).

Notes and references

1 (a) M. W. Urban (Ed.), *Handbook of Stimuli-Responsive Materials*, Wiley-VCH, Weinheim, Germany, 2011, 1–278; (b) P. Theato, B. S. Sumerlin, R. K. O'Reilly, T. H. Epps, III, *Chem. Soc. Rev.*, 2013, **42**, 7055–7056.

2 S. Horike, S. Shimomura, S. Kitagawa, *Nat. Chem*., 2009, **1**, 695−704.

3 (a) O. Sato, J. Tao, Y. Z. Zhang, Angew. *Chem. Int. Ed.*, 2007, **46**, 2152–2187; (b) O. Sato, *Nat. Chem*., 2016, **8**, 644−656.

4 (a) S. Horiuchi, Y. Tokura, *Nat. Mater.*, 2008, **7**, 357−366; (b) W. Zhang, R.-G. Xiong, *Chem. Rev.,* 2012, **112**, 1163−1195.

5 C. Shi, X.-B. Han, W. Zhang, *Coord. Chem. Rev.*, 2017, https://doi.org/10.1016/j.ccr.2017.09.020.

6 (a) W. Zhang, Y. Cai, R.-G. Xiong, H. Yoshikawa, K. Awaga, *Angew. Chem. Int. Ed.*, 2010, **49**, 6608−6610; (b) W. Zhang, H.-Y. Ye, R. Graf, H. W. Spiess, Y.-F. Yao, R.-Q. Zhu, R.-G. Xiong, *J. Am. Chem. Soc.*, 2013, **135**, 5230−5233; (c) X. Zhang, X.-D. Shao, S.-C. Li, Y. Cai, Y.-F. Yao, R.-G. Xiong, W. Zhang, *Chem. Commun.* 2015, **51**, 4568−4571; (d) C. Shi, C.-H. Yu, W. Zhang, *Angew. Chem. Int. Ed.*, 2016, **55**, 5798−5802.

7 (a) B. Wei, R. Shang, X. Zhang, X.-D. Shao, Y.-F. Yao, Z.-M. Wang, R.-G. Xiong, W. Zhang, *Chem. Eur. J.*, 2014, **20**, 8269−8273; (b) C. Shi, X. Zhang, Y. Cai, Y.-F. Yao, W. Zhang, *Angew. Chem. Int. Ed.*, 2015, **54**, 6206−6210; (c) Y.-L. Liu, W. Zhang, *Chem. Commun.*, 2017, **53**, 6077−6080.

8 (a) P. Hu, R.-Q. Zhu, W. Zhang, *Polyhedron*, 2016, **115**, 137–141; (b) X.-H. Yuan, X.-D. Shao, C. Shi, W. Zhang, *Inorg. Chem. Commun.*, 2016, **67**, 35−39; (c) Y.-L. Liu, Y.-F. Wang, W. Zhang, *CrystEngComm*, 2016, **18**, 1958−1963; (d) Y.-L. Liu, W. Zhang, *Inorg. Chem. Front.*, 2017, **4**, 1304−1310; (e) C. Shi, Y. Wang, X.-B. Han, W. Zhang, *Eur. J. Inorg. Chem.*, 2017, 3685−3689.

9 (a) P. Jain, V. Ramachandran, R. J. Clark, H. D. Zhou, B. H. Toby, N.S. Dalal, H. W. Kroto, and A. K. Cheetham, *J. Am. Chem. Soc.*, 2009, **131**, 13625−13627; (b) R. Shang, G.C. Xu, Z.M. Wang, S. Gao, *Chem. Eur. J.*, 2014, **20**, 1146−1158; (c) R. Shang, S. Chen, K. L. Hu, Z. C. Jiang, B. W. Wang, M. Kurmoo, Z. M. Wang, S. Gao, *APL Mater*., 2014, **2**, 124104; (d) R. Shang, Z.M. Wang, S. Gao, *Angew. Chem. Int. Ed.*, 2015, **54**, 2534−2537; (e) R. Shang, S. Chen, K.L. Hu, Z.M. Wang, S. Gao, *Chem. Eur. J.*, 2016, **22**, 6199−6203.

10 a) C.-M. Ji, Z.-H. Sun, S.-Q. Zhang, T.-L. Chen, P. Zhou, J.-H. Luo, *J. Mater. Chem. C.* 2014, **2**, 567−572; b) Z.-Y. Du, T.-T. Xu, B. Huang, Y.-J. Su, W. Xue, C.-T. He, W.-X. Zhang, X.-M. Chen, *Angew. Chem. Int. Ed*., 2015, **54**, 914−918.

11 (a) W. Q. Liao, G. Q. Mei, H. Y. Ye, Y. X. Mei, Y. Zhang, *Inorg. Chem.*, 2014, **53**, 8913–8918; (b) Z. X. Wang, W. Q. Liao, H. Y. Ye, Y. Zhang, *Dalton Trans*., 2015, **44**, 20406–20412; (c) X. H. Lv, W. Q. Liao, P. F. Li, Z. X. Wang, C. Y. Mao, Y. Zhang, *J. Mater. Chem. C.*, 2016, **4**, 1881–1885; (d) X. F. Sun, Z. X. Wang, P. F. Li, W. Q. Liao, H. Y. Ye, Y. Zhang, *Inorg. Chem.*, 2017, **56**, 3506–3511.

12 (a) D. B. Mitzi, *Prog. Inorg. Chem.* 1999, **48**, 1–121; (b) W. J. Xu, Z. Y. Du, W. X. Zhang, X. M. Chen, CrystEngComm, 2016, **18**, 7915–7928.

13 H. Fröhlich, Theory of Dielectrics; Oxford University Press: Oxford, U.K., 1991.

14 Y.-L. Sun, X.-B. Han, W. Zhang, *Chem. Eur. J.*, 2017, **23**, DOI: 10.1002/chem.201702228.

15 (a) O. Delgado-Friedrichs, M. O'Keeffe, O. M. Yaghi, *Acta Crystallogr. A,* 2006, **62**, 350–355; (b) M. Li, D. Li, M. O'Keeffe, O. M. Yaghi, *Chem. Rev.*, 2014, **114**, 1343–1370.

16 A. L. Spek, *Acta Crystallogr. Sect. D*, 2009, **65**, 148–155.

17 M. Wojtaś, A. Gągor, O. Czupiński, A. Piecha-Bisiorek, D. Isakov, W. Medyckid, R. Jakubas, *CrystEngComm*, 2015, **17**, 3171–3180.

18 (a) Y. Zhang, Y.-M. Liu, H.-Y. Ye, D.-W. Fu, W.-X. Gao, H. Ma, Z.-G. Liu, Y.-Y. Liu, W. Zhang, J.-Y. Li, G.-L. Yuan, R.-G. Xiong, *Angew. Chem. Int. Ed.*, 2014, **53**, 5064−5068; (b) X.-D. Shao, X. Zhang, C. Shi, Y.-F. Yao and W. Zhang, *Adv. Sci.*, 2015, **2**, 1500029; (c) M. Wojtaś, A. Gągor, A.L. Kholkin, *J. Mater. Chem. C*, 2016, **4**, 7622−7631.

19 (a) M. A. Garcia-Garibay, *Proc. Natl. Acad. Sci. USA*, 2005, **102**, 10771−10776; (b) C. S. Vogelsberg, M. A. Garcia-Garibay, *Chem. Soc. Rev.*, 2012, **41**, 1892–1910; (c) S. D. Karlen, H. Reyes, R. E. Taylor, S. I. Khan, M. F. Hawthorne and M. A. Garcia-Garibay, *Proc. Natl. Acad. Sci. USA*, 2010, **107**, 14973−14977.

20 (a) C. Lemouchi, C. S. Vogelsberg, L. Zorina, S. Simonov, P. Batail, S. Brown, M. A. Garcia-Garibay, *J. Am. Chem. Soc.*, 2011, **133**, 6371–6379; (b) C. Lemouchi, K. Iliopoulos, L. Zorina, S. Simonov, P. Wzietek, T. Cauchy, A. Rodríguez-Fortea, E. Canadell, J. Kaleta, J. Michl, D. Gindre, M. Chrysos, P. Batail, *J. Am. Chem. Soc.*, 2013, **135**, 9366–9376.

21 (a) G. S. Kottas, L. I. Clarke, D. Horinek, J. Michl, *Chem. Rev.*, 2005, **105**, 1281–1376. (b) T. Akutagawa, H. Koshinaka, D. Sato, S. Takeda, S.-I. Noro, H. Takahashi, R. Kumai, Y. Tokura, T. Nakamura, *Nat. Mater.*, 2009, **8**, 342–347.